AN IN-FLIGHT RADIOACTIVE ION SEPARATOR DESIGN FOR THE ATLAS FACILITY*

B. Mustapha[#], C.R. Hoffman, B.P. Kay, B.B. Back, J.A. Nolen and P.N. Ostroumov
Physics Division, ANL, Argonne, IL 60439, USA

Abstract

An in-flight radioactive beam separator, named AIRIS, is being designed to enhance the radioactive beam capabilities of the ATLAS facility at Argonne. In order to serve all the experimental areas while maintaining the stable beam capabilities, the separator design is of a broadband type. This design allows the selected radioactive beam to return to the ATLAS beam line while stable beams continue on the same straight line when the separator is turned off. The separation is performed in two steps. The first is magnetic in a chicane made of four magnets and four multipoles, while the second uses an rf sweeper taking advantage of the time separation between the beam of interest and potential contaminants including the primary beam tail. We report here on the progress of the AIRIS design effort with special emphasis on the performance of the rf sweeper.

AIRIS LAYOUT AND DESIGN PARAMETERS

An efficiency and intensity upgrade of the ATLAS accelerator facility at Argonne has just been successfully completed [1]. Most of the stable beams will see their intensities increased by one to two orders of magnitude. To take advantage of this intensity upgrade and to enhance the existing radioactive beam capability at ATLAS [2], a new in-flight radioactive beam production and separation system is being designed. The new system will consist of a production target placed at the end of ATLAS followed by a two-step ion separator. The first step is magnetic called AIRIS while the second consists of an RF sweeper or chopper to take advantage of the time separation of the selected beam from potential contaminants including the tail of the primary beam, which could be orders of magnitude more intense. Figure 1 shows how AIRIS and the rf sweeper will be integrated into the ATLAS facility following the last accelerating module. The main constraint on the AIRIS design is to preserve stable beam operation by moving the target out

and using AIRIS as a zero-degree transport line. For this purpose, AIRIS should have the same beam axis as ATLAS and the existing beamline. The developed design is of broadband type [3, 4] made of 4 rectangular dipoles and four quadrupoles. Table 1 lists the most recent AIRIS design parameters.

Table 1: AIRIS Design Parameters

Parameter	Value
Total chicane length, m	6.6
Angular acceptance, mrad	75
Dispersion at mid-plane, mm/%	1.2
Dipole bend angle, deg	22.5
Dipole radius, m	1
Dipole full gap, cm	8
Max. dipole field, T	1.8
Quadrupole length, cm	30
Quadrupole full aperture, cm	16
Max. quad. field at pole-tip, T	1.1

AIRIS INTEGRATION INTO ATLAS

As shown in figure 1, AIRIS will be installed downstream of the last ATLAS cryomodule and upstream of all experimental areas to maximize the use of ATLAS beams. In the original configuration, the rf sweeper was located just downstream of AIRIS in front of the first switching magnet. Due to space limitations in the ATLAS tunnel, the rf sweeper was moved downstream of the switching magnet preventing one or two experimental areas from taking advantage of the time separation provided by the sweeper. As we will show later, the new sweeper location has a significant advantage by providing a much better time separation due to the longer beam path between AIRIS and the sweeper.
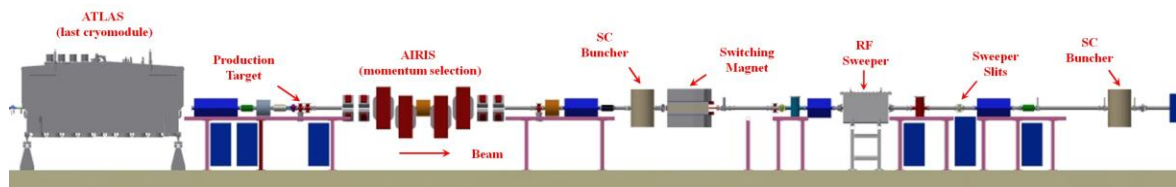
Figure 1: Integration of AIRIS and the RF sweeper into the ATLAS facility following the last accelerating module.

THE RF SWEEPER EEFECT

Figure 2 shows how the $^{56}Ni^{27+}$ beam could not be spatially separated from the $^{55}Co^{27+}$ contaminant in AIRIS due to their close magnetic rigidity. At the same time, we can see a clear time separation between the two beams at the AIRIS exit due to their velocity difference. The time separation gets larger at the sweeper due to the long path travelled by the beams. Using the appropriate phase and voltage setting for the sweeper, we can apply an angular kick to the $^{55}Co^{27+}$ contaminant while the $^{56}Ni^{27+}$ beam of interest remains unaffected. The angular kick translates into a position separation at the slits placed 2 m downstream of the sweeper where a selection can be made for a purer $^{56}Ni^{27+}$ beam.
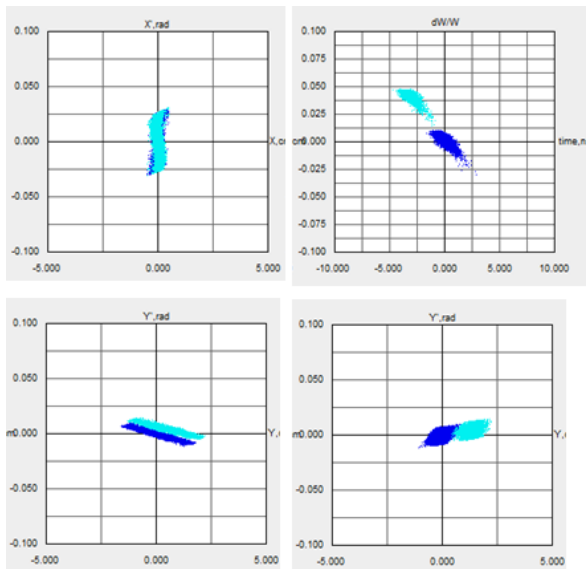
Figure 2: Top-left: the $^{56}Ni^{27+}$ beam (blue) is not magnetically separated from the $^{55}Co^{27+}$ contaminant (cyan) in AIRIS. Top-right: A clear time separation between them due to velocity difference. Bottom-left: $^{55}Co^{27+}$ receives an angular kick in the sweeper. Bottom-right: the angular kick becomes a clear position separation at the slits.

THE SWEEPER LOCATION

As mentioned above, the original sweeper location was just upstream of the first switching magnet and it was moved downstream due to tight space constraints in the ATLAS tunnel. Figure 3 shows a comparison of the results for the two sweeper locations before and after moving it. As can be seen, the longer beam path creates a larger time separation which means lower sweeper voltage requirement to produce the same angular kick. The result is a much better position separation at the slits which was not achieved in the original location at the maximum sweeper voltage. The new location is about 5 m downstream of the switching magnet and allows plenty of space to place a doublet in front of the sweeper to focus
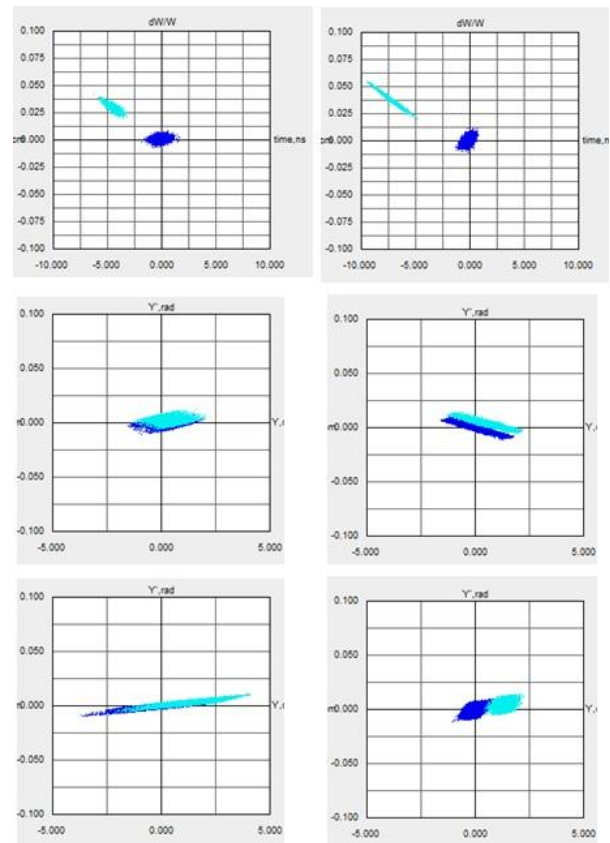
Figure 3: Comparison of the two sweeper locations, the plots on the left are for the original location, those on the right are for the new location. The top plots show the time separation at the sweeper, the middle ones show the angular kick right after the sweeper and the bottom ones show the physical separation achieved at the slits.

the beam on the slits for tighter and cleaner selection. A new triplet was also added after the slits for better capture and transmission of the selected beam. We noticed up to 15% improvement in beam transmission after introducing these modifications in the beam line. At this location, the sweeper will not serve all the experimental areas, but if needed a similar system could be installed for other beam lines.

EXAMPLES OF COMBINED AIRIS AND RF SWEEPER PERFORMANCE

AIRIS will be used to produce beams of radioactive isotopes in the 5-15 MeV/u energy range for nuclear astrophysics, nuclear structure and reaction studies. AIRIS mass resolution depends on the production reaction kinematics, but it should be able to produce and separate beams up to mass 60. The first main challenge of AIRIS is to get rid of the primary beam core in the middle focal plane. The primary beam tail and other potential contaminants should be eliminated or minimized in the RF sweeper. The purity of a beam will depend significantly on the choice of the production reaction and the selected charge state. These choices may affect the intensity of the secondary beam. In cases where the beam intensity is more

important than its purity, a different reaction with a higher cross section and higher charge state fraction could be selected. In the following we present examples showing the performance of the AIRIS and rf sweeper combination for typical beams at different energies.

Case of ^{14}O from ^{14}C (p, n) at 15 MeV/u

Figure 4 shows how the primary ^{14}C beam core could be eliminated in the AIRIS mid-plane (top 3 plots) while its tail could not. The figure also show the time separation between the selected ^{14}O beam and the ^{14}C beam tail which was exploited by the rf sweeper to apply an angular kick to the ^{14}C beam tail to be completely eliminated at the sweeper slits downstream.
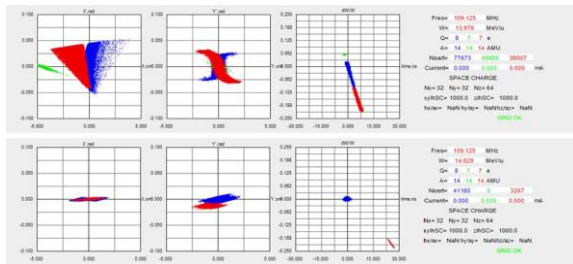
Figure 4: The top 3 plots show the phase space at the AIRIS mid-plane while the bottom 3 plots show the phase space right after the sweeper.

Case of ^{50}Ca from ^{48}Ca (+2n) at 10 MeV/u

By applying tight slits in AIRIS mid-plane, we were able to eliminate both the primary ^{48}Ca beam core and tail, but not the ^{49}Ca contaminant which could be several times more important than the ^{50}Ca beam of interest. Figure 5 shows the phase space plots at the AIRIS mid-plane and after the sweeper. We can see that the time separation of ^{50}Ca and ^{49}Ca is not enough for the sweeper to completely eliminate ^{49}Ca but it was suppressed by a significant factor, 2500 times in this case.
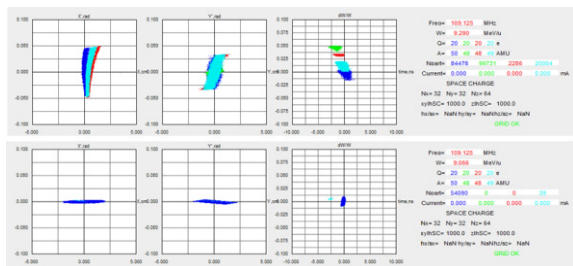
Figure 5: The top 3 plots show the phase space at the AIRIS mid-plane while the bottom 3 plots show the phase space right after the sweeper.

Case of ^{25}Al from ^{24}Mg (d, n) at 5 MeV/u

In this case we notice a clear separation of the ^{24}Mg beam core from the ^{25}Al beam in the AIRIS mid-plane. The primary beam tail and other contaminants are yet to be investigated. At this lower energy, the velocity difference between the different beam components is large enough to produce a good time separation at the sweeper. Also at this energy the beam tails are more extended and more charge

states are populated. These two factors will affect both the transmission and purity of these low-energy beams. As can be seen in Figure 6, the extended phase space of the ^{25}Al beam results in poor beam quality and lower overall transmission than what was observed at higher energies. Table 2 lists the transmission and purity of selected beams with different masses at different energies. It is important to mention that the transmission depends in large part on the kinematics of the production reaction.
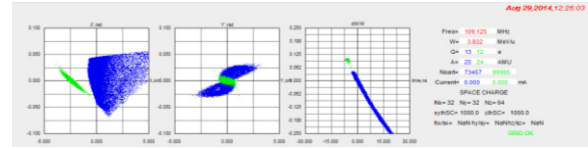
Figure 6: Phases space plots at the AIRIS mid-plane for ^{25}Al (blue) and the ^{24}Mg primary beam core (green).

Table 2: Transmission and purity of selected beams

Beam	Beam Energy (MeV/u)	End of AIRIS (%)	End of Beamline (%)	Estimated Purity (%)
$^{14}O^{8+}$	14.0	72	30	100
$^{50}Ca^{20+}$	9.1	80	54	90
$^{56}Ni^{28+}$	8.6	89	50	100
$^{56}Ni^{27+}$	8.6	88	49	90
$^{25}Al^{13+}$	3.8	48	17	60

As mentioned above, the transmission depends on the kinematics and the beam quality while the purity depends on the products and charge states produced in the same reaction. We notice in particular the case of the $^{56}Ni^{28+}$ and $^{56}Ni^{27+}$ beams, while $^{56}Ni^{28+}$ is purer, $^{56}Ni^{27+}$ is about ten times stronger. This is an example of compromising between the purity and intensity of the selected radioactive beam.

REFERENCES

[1] P.N. Ostroumov et al, "Completion of Efficiency and Intensity Upgrade of the ATLAS Facility", These Proceedings, paper TUPP005.

[2] B. Harss et al., "Production of radioactive ion beams using the in-flight technique", Rev. Sci. Instr. 71 (2000) 380.

[3] S. Manikonda et al., "Argonne In-flight Radioactive Ion Separator", Proceedings of HIAT-2012, Chicago, IL, USA.

[4] B. Mustapha et al, "Design and Simulation of AIRIS", Proceedings of NA-PAC 2013, Pasadena, CA, p 351.

02 Proton and Ion Accelerators and Applications

2G Other Proton/Ion